Journal of Natural and Artificial Scientific Systems, 2026, 3(2): 238-256

YOLO26-Based Framework for Automated Liver Cancer Detection and Localization in CT Images

Muhammad Jamilu Muhammad, Anas Tukur Balarabe, Bashar Aliyu Yauri, Hassan Umar Suru and Abdulrashid Sani

Received: 19 March 2026/Accepted: 20 June 2026/Published: 24 June 2026

Abstract: *Liver cancer remains a major global health challenge due to the difficulty of early and accurate diagnosis from medical images. This study presents a YOLO26-based deep learning framework for automated liver cancer detection using Computed Tomography (CT) scan images. The proposed framework performs simultaneous lesion localization and classification within an end-to-end object detection pipeline. Approximately 12,000 annotated CT images were utilized for model training and evaluation following preprocessing and annotation preparation. Experimental results showed that the model achieved a Precision of 0.9600, Recall of 0.9257, F1-score of 0.9425, and mAP@0.5 of 0.9600, indicating strong detection and localization performance. Qualitative evaluation further demonstrated effective localization of suspicious liver lesions across different CT image samples. Compared with several existing approaches, the proposed framework showed improved localization consistency and enhanced small lesion detection capability. A Gradio-based deployment environment was also implemented to validate real-time inference on unseen CT images. The findings suggest that YOLO26 provides a promising approach for automated liver cancer detection and computer-aided medical imaging applications.*

Keywords: *Liver Cancer Detection, YOLO26, Deep Learning, Computed Tomography (CT), Hepatocellular Carcinoma (HCC)*

Muhammad Jamilu Muhammad
Department of Computer Science, Faculty of Computing, Sokoto State University, Sokoto State, Nigeria.
Email: minajameel@gmail.com.
https://orcid.org/0009-0003-1605-8856

Anas Tukur Balarabe
Department of Computer Science, Faculty of Computing, Sokoto State University, Sokoto State, Nigeria.
Email: anas.balarabe@ssu.edu.ng.
https://orcid.org/0000-0001-7739-4616

Bashar Aliyu Yauri
Department of Computer Science, Faculty of Computing, Abdullahi Fodio University of Science and Technology, Aliero, Kebbi State, Nigeria.
Email: bashar.aliyu@ksusta.edu.ng.
https://orcid.org/0000-0002-9953-6213

Hassan Umar Suru
Department of Computer Science, Faculty of Computing, Abdullahi Fodio University of Science and Technology, Aliero, Kebbi State, Nigeria.
Emai. hu.suru@ksusta.edu.ng.
https://orcid.org/0009-0009-9249-3896

Abdulrashid Sani
Department of Computer Science, Faculty of Computing, Sokoto State University, Sokoto State, Nigeria.
Email: abdulrashid.sani@ssu.edu.ng.
ttps://orcid.org/0009-0000-9033-786X

1.0 Introduction

Liver cancer is one of the leading causes of cancer-related morbidity and mortality worldwide, posing a significant public health challenge due to its increasing incidence and

poor prognosis when diagnosed at advanced stages (Wu *et al*., 2024). Among the various forms of liver cancer, hepatocellular carcinoma (HCC) accounts for approximately 75–85% of all primary liver cancer cases and remains the most prevalent malignant liver tumor globally (Amin *et al*., 2025). Despite substantial advances in cancer diagnosis and treatment, liver cancer continues to exhibit high mortality rates because early-stage tumors often develop without obvious clinical symptoms, resulting in delayed diagnosis and limited therapeutic options (Hu, 2026). Consequently, the development of accurate and reliable early detection systems has become a critical area of research aimed at improving patient survival and treatment outcomes.

Medical imaging technologies play a fundamental role in the diagnosis, staging, and monitoring of liver cancer. Among these technologies, Computed Tomography (CT) imaging is widely utilized because it provides high-resolution visualization of liver tissues, vascular structures, and tumor morphology, enabling clinicians to assess lesion characteristics and disease progression effectively (Luu *et al*., 2024; Huang *et al*., 2024). However, manual interpretation of CT images remains a challenging and time-intensive task. Factors such as low contrast between healthy and malignant tissues, image noise, variations in tumor size and shape, overlapping anatomical structures, and inter-observer variability can significantly affect diagnostic accuracy (Tatar *et al*., 2025; Shen *et al*., 2025). Small lesions, in particular, are often difficult to identify, increasing the likelihood of missed diagnoses and delayed treatment initiation.

Recent advances in Artificial Intelligence (AI), machine learning, and deep learning have transformed medical image analysis by enabling automated detection, classification, and localization of pathological abnormalities with high accuracy (Sankuru *et al*., 2026; Osman, 2026). Deep learning models, particularly Convolutional Neural Networks (CNNs), have demonstrated remarkable success in extracting complex image features directly from medical images without the need for handcrafted feature engineering (Rahoma *et al*., 2024). These capabilities have facilitated the development of Computer-Aided Diagnosis (CAD) systems capable of supporting radiologists in disease detection and clinical decision-making.

Within the domain of medical image analysis, object detection models have emerged as powerful tools for simultaneously identifying and localizing abnormalities in diagnostic images. The You Only Look Once (YOLO) family of object detectors has gained widespread attention due to its ability to perform real-time object detection through a single-stage detection mechanism, thereby combining speed and accuracy in a unified framework (Sun, 2025; Review & Previous, 2025). Successive YOLO versions have introduced significant improvements in feature extraction, multi-scale detection, computational efficiency, and small-object recognition, making them increasingly suitable for medical imaging applications where precise lesion localization is required (Li, 2024; Sidi *et al*., 2026). Recent studies have demonstrated the effectiveness of YOLO-based architectures in detecting tumors and lesions across various imaging modalities, including CT, MRI, and ultrasound images (Huang, 2024; Karabağ *et al*., 2026).

The evolution of automated liver cancer detection has progressed from conventional image processing techniques to sophisticated deep learning and object detection frameworks. Early studies relied heavily on image enhancement, thresholding, segmentation, and handcrafted feature extraction methods to identify liver tumors from CT images. For example, Moghimhanjani & Taghavirashidizadeh (2022.) employed Otsu

thresholding, marker-controlled watershed segmentation, and Self-Organizing Maps (SOM) for tumor identification and boundary extraction. While these approaches demonstrated the feasibility of automated liver lesion analysis, their performance was highly sensitive to image noise, low contrast, and anatomical variability, limiting their practical clinical applicability.

The emergence of deep learning significantly improved the accuracy and robustness of liver cancer diagnosis systems. Rahoma *et al*. (2024) developed an automated liver cancer detection framework using U-Net and ResNet architectures with transfer learning, reporting a classification accuracy of 96% and a Dice similarity coefficient of 0.926. Similarly, Badrawy *et al*. (2024) highlighted the effectiveness of artificial intelligence techniques in improving liver cancer diagnosis through enhanced feature learning and pattern recognition. Despite these improvements, challenges associated with low-contrast lesions and heterogeneous imaging conditions remained unresolved.

Recent studies have explored hybrid and ensemble learning approaches to further improve diagnostic performance. Vamsy *et al*. (2026) proposed CT-LiverNet, an efficient deep learning model for liver lesion segmentation and diagnosis, demonstrating promising performance in lesion identification and classification. Likewise, Alqaralleh *et al*. (2026) introduced an intelligent healthcare framework that combined aggregated learning models with Explainable Artificial Intelligence (XAI) techniques to improve both diagnostic accuracy and interpretability, achieving an accuracy of 98.18%. Although these approaches improved classification performance, many focused primarily on lesion classification rather than precise lesion localization.

Advancements in medical object detection have increasingly emphasized accurate tumor localization and small lesion detection. Li (2024) proposed a modified YOLOv8 architecture for liver tumor detection in abdominal CT scans, reporting improved localization accuracy compared with conventional CNN-based methods. Similarly, Li (2025) developed PCA-YOLO, which incorporated a Patch-Contrastive Attention mechanism to enhance the detection of small liver tumors. The model demonstrated superior performance in identifying tumors as small as 0.4 cm; however, challenges related to lesion merging, splitting errors, and spatial differentiation persisted.

Other studies have explored YOLO-based approaches in different medical imaging domains. Huang (2024) successfully applied YOLO for liver ultrasound lesion detection, while Zhou *et al*. (2025) proposed a deep learning detect-then-track framework for assessing treatment outcomes in immunotherapy-treated liver cancer patients. Furthermore, Sidi *et al*. (2026) demonstrated the effectiveness of YOLOv8 for liver tumor detection, highlighting the potential of modern object detection architectures in clinical imaging applications. These studies collectively indicate that YOLO-based frameworks have become increasingly important for medical image analysis due to their balance between detection speed and accuracy.

Despite the significant progress achieved in automated liver cancer diagnosis, several challenges remain unresolved. First, many existing studies focus predominantly on segmentation or classification tasks without simultaneously addressing accurate lesion localization and detection. Second, the detection of small tumors remains difficult due to low image contrast, irregular lesion boundaries, and substantial variations in tumor appearance across CT datasets (Li, 2025; Tatar *et al*., 2025). Third, several state-of-the-art models employ complex multi-stage

architectures that increase computational requirements and limit real-time deployment capabilities in clinical environments. Furthermore, many existing frameworks have demonstrated reduced generalization performance when applied to heterogeneous CT datasets acquired under varying imaging conditions (Alqaralleh *et al*., 2026; Huang *et al*., 2024).

Although YOLO-based models such as YOLOv8 have shown promising performance in liver tumor detection, limited studies have investigated the application of the recently developed YOLO26 architecture for automated liver cancer detection in CT imaging. YOLO26 introduces architectural enhancements designed to improve feature representation, detection accuracy, computational efficiency, and small-object recognition capabilities (Sapkota *et al*., 2026; Sani *et al*., 2026). However, its effectiveness in liver cancer detection remains largely unexplored within the existing literature. This gap necessitates a comprehensive evaluation of YOLO26 for accurate and efficient liver lesion detection in CT images.

The primary aim of this study is to evaluate the effectiveness of the YOLO26 object detection architecture for automated liver cancer detection using CT scan images.

To achieve this aim, the study seeks to:

1. Develop a YOLO26-based liver cancer detection model using annotated CT scan datasets.
2. Train and evaluate the model for accurate liver lesion localization and detection.
3. Assess model performance using Precision, Recall, F1-Score, and Mean Average Precision (mAP) metrics.
4. Implement a Gradio-based deployment interface for real-time inference and visualization of detection results.
5. Compare the detection capability of YOLO26 with findings reported in existing liver cancer detection studies.

This study contributes to the growing field of artificial intelligence-assisted medical diagnosis by investigating the applicability of the recently developed YOLO26 architecture for liver cancer detection. The findings are expected to provide insights into the suitability of advanced object detection models for clinical imaging applications, particularly in detecting and localizing liver tumors from CT scans. By improving detection accuracy and reducing dependence on manual image interpretation, the proposed framework can support radiologists in early diagnosis and treatment planning. Furthermore, the integration of a Gradio-based deployment environment demonstrates the practical feasibility of translating deep learning research into user-friendly clinical decision-support tools.

The study also contributes to the existing body of knowledge on medical object detection by providing empirical evidence on the performance of YOLO26 in a healthcare context. Given the increasing demand for accurate, efficient, and deployable AI solutions in medical imaging, the outcomes of this research may facilitate the development of next-generation computer-aided diagnostic systems for liver cancer and related oncological applications.

Table 1 provides a comparative summary of major liver cancer detection studies and highlights the research gaps that motivate the present study.

2.0 Methodology

2.1 Research Design

This study adopted a deep learning-based computer vision research design for the automated detection and localization of liver cancer lesions from Computed Tomography (CT) scan images. The study was designed to evaluate the performance of the YOLO26

object detection architecture in identifying malignant liver lesions and providing accurate spatial localization within medical images. Recent advancements in the YOLO family of object detection models have demonstrated significant improvements in detection accuracy, computational efficiency, and real-time inference capabilities, making them suitable for medical imaging applications requiring rapid and accurate diagnosis (Review & Previous, 2025; Sapkota *et al*., 2026).

Table 1: Summary of Related Works

Source	Methodology / Architecture	Key Findings	Identified Research Gaps
Li (2025)	PCA-YOLO framework integrating Patch-Contrastive Attention (PCA) with a YOLOv8x detection head	Achieved 77.2% mAP@50% and improved detection of tumors as small as 0.4 cm	Experienced lesion merging and splitting errors, limiting detection reliability for clinically challenging small tumors
Vamsy *et al*. (2026)	Hybrid ensemble framework combining YOLO feature extraction with RFE, Random Forest, and XGBoost	Achieved 97.18% precision through enhanced hierarchical feature extraction	Primarily focused on binary classification and feature extraction with limited robustness across varying pathological tissue conditions
Moghimhanjani and Taghavirashidizadeh (n.d.)	Conventional image processing using Otsu's thresholding, Watershed Segmentation, wavelet transforms, and SOM	Demonstrated automated tumor segmentation feasibility using multi-resolution image analysis	Performance significantly affected by image noise, low contrast, and structural variability
Rahoma *et al*. (2024)	Transfer learning with U-Net and ResNet	ResNet achieved 96% accuracy and Dice score of 0.926	Difficulty distinguishing malignant tissues from healthy liver regions
Badrawy *et al*. (2024)	Decision fusion framework integrating VGG19, ResNet50, and LTHR-Net	Achieved 99.9% classification accuracy	Limited generalization across clinical environments
Alqaralleh *et al*. (2026)	HCDAL-XAI framework combining SAE, GRU, DBN, and SHAP	Achieved 98.18% accuracy with explainability	Limited multimodal integration and insufficient validation

The research framework consisted of six major phases: dataset acquisition, image preprocessing, annotation preparation, model training, model evaluation, and deployment. The entire workflow was implemented using Python-based deep learning libraries, including PyTorch and Ultralytics, with GPU-accelerated computation to enhance training efficiency, reduce computational time, and improve experimental reproducibility (Sani *et al*., 2026; Sapkota *et al*., 2026).

The proposed framework employed an end-to-end object detection strategy in which liver CT images were directly supplied to the YOLO26 architecture for simultaneous lesion localization and classification. Unlike traditional computer-aided diagnosis systems that separately perform feature extraction, segmentation, and classification, YOLO26 integrates these processes into a unified detection framework, thereby reducing computational complexity and improving inference speed (Review & Previous, 2025). The effectiveness of the developed model was evaluated using Precision, Recall, F1-Score, and Mean Average Precision (mAP), which are widely adopted performance metrics for object detection systems (Sidi *et al*., 2026). Furthermore, a Gradio-based deployment interface was developed to validate the practical applicability of the trained model on previously unseen CT images.

2.2 System Architecture

The proposed liver cancer detection framework was implemented as an integrated deep learning pipeline comprising data acquisition, preprocessing, feature extraction, lesion localization, classification, and deployment stages. The overall architecture commenced with the acquisition of annotated liver CT images, followed by image preprocessing operations such as normalization, resizing, and annotation formatting to ensure compatibility with the YOLO26 detection framework.

Following preprocessing, the standardized CT images were supplied to the YOLO26 model for feature extraction and lesion detection. The backbone network extracted hierarchical features representing tissue texture, lesion boundaries, structural abnormalities, and spatial characteristics associated with malignant liver tissues. These extracted features were subsequently forwarded to the neck network, where feature fusion and aggregation were performed across multiple scales. Multi-scale feature aggregation has been shown to improve the detection of small and irregular tumors that frequently occur in liver cancer imaging datasets (Huang *et al*., 2024; Li, 2025).

The detection head simultaneously generated lesion classification outputs, confidence scores, and bounding box coordinates within a single forward pass. This architecture enabled the model to perform localization and classification concurrently, thereby improving detection efficiency and reducing inference latency. The final predictions were visualized through a Gradio-based deployment interface that allowed users to upload CT images and obtain automated liver cancer detection results, including lesion locations and associated confidence scores. The modular design of the framework further enabled independent optimization of preprocessing, training, and deployment stages while maintaining overall system integration.

The liver CT images utilized in this study were obtained from publicly available medical imaging repositories developed for liver lesion analysis, liver tumor segmentation, and hepatocellular carcinoma detection research. Publicly available datasets have become important resources for developing and evaluating artificial intelligence-based diagnostic systems due to their diversity and standardized annotations (Luu *et al*., 2024; Huang *et al*., 2024).

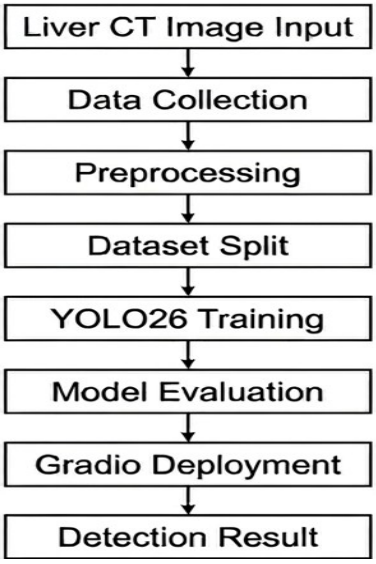

Fig. 1: Research Architecture

2.3 Data Collection and Sampling

The dataset consisted of approximately 12,000 annotated CT images representing multiple liver cancer conditions and varying lesion characteristics, including differences in size, shape, texture, contrast, and anatomical location. The utilization of a relatively large and heterogeneous dataset was intended to improve model generalization, reduce overfitting, and enhance robustness across different imaging conditions. Each image was accompanied by lesion annotations indicating the spatial location of cancerous regions, thereby facilitating supervised learning and object detection training.

2.4 Image Preprocessing

Prior to model training, several preprocessing operations were performed to improve image consistency, enhance training stability, and ensure compatibility with the YOLO26 architecture. Image preprocessing is a critical step in deep learning-based medical image analysis because it reduces variability arising from different imaging equipment, acquisition protocols, and patient-specific characteristics (Rahoma *et al*., 2024; Tatar *et al*., 2025).

2.4.1 Annotation and Bounding Box Generation

Expert-provided lesion annotations were converted into YOLO-compatible bounding box formats using normalized coordinate values. These annotations enabled the model to learn the spatial characteristics and locations of malignant liver lesions during supervised training. Bounding box annotation remains one of the most effective methods for training object detection models in medical imaging applications (Li, 2025; Alqaralleh *et al*., 2026).

2.4.2 Image Resizing

All CT images and their corresponding annotation coordinates were resized to an input resolution of 1024 × 1024 pixels. The selected resolution was intended to preserve fine-grained anatomical details and improve the detection of small lesions that could otherwise be lost at lower image resolutions. Previous studies have demonstrated that higher-resolution inputs significantly enhance small-object detection performance in medical imaging tasks (Huang, 2024; Li, 2025).

2.4.3 Dataset Splitting

Following preprocessing, the dataset was divided into training, validation, and testing subsets using a ratio of 70%, 15%, and 15%, respectively. This partitioning strategy ensured that model training, hyperparameter tuning, and performance evaluation were conducted on independent datasets, thereby minimizing data leakage and improving experimental reliability. Similar dataset partitioning strategies have been widely adopted in medical image analysis studies (Sidi *et al*., 2026; Rahoma *et al*., 2024).

2.5 YOLO26 Model Description and Training

This study employed the YOLO26 object detection architecture as the primary deep learning framework for automated liver cancer detection. YOLO26 belongs to the latest generation of the YOLO family of object detectors and was developed to improve object localization accuracy, computational

efficiency, and small-object detection performance (Sapkota *et al*., 2026). Similar to earlier YOLO variants, YOLO26 performs object localization and classification simultaneously within a single inference process, enabling end-to-end object detection without requiring separate region proposal stages (Review & Previous, 2025).

A major architectural advancement of YOLO26 is its Non-Maximum Suppression (NMS)-free detection mechanism. Traditional object detectors commonly utilize NMS as a post-processing operation to remove duplicate predictions; however, YOLO26 incorporates direct prediction optimization within the network architecture, thereby reducing prediction redundancy and improving localization consistency (Sapkota *et al*., 2026). This enhancement is particularly beneficial in medical imaging environments where precise lesion localization is critical for clinical decision-making.

The detection process begins by supplying preprocessed liver CT images to the backbone network responsible for extracting hierarchical image features. These features include tissue textures, lesion boundaries, abnormal anatomical structures, and spatial patterns associated with malignant liver regions. The extracted features are subsequently forwarded to the neck architecture, where multi-scale feature fusion is performed to combine low-level spatial information with high-level semantic representations. Multi-scale feature learning improves the model's ability to detect both large tumors and subtle lesions exhibiting low contrast characteristics (Karabağ *et al*., 2026; Huang *et al*., 2024).

The detection head simultaneously predicts lesion classes, confidence scores, and bounding box coordinates. This integrated architecture enables efficient lesion localization and classification while maintaining real-time inference capability. The model was trained for 100 epochs using GPU acceleration with a batch size of 16 and adaptive learning rate scheduling to improve convergence stability. During training, localization loss, classification loss, and confidence loss were iteratively minimized to optimize detection performance.

Following model training, the best-performing weight file obtained during validation was integrated into a Gradio-based deployment environment for real-time inference. The deployment interface allows clinicians and researchers to upload unseen liver CT images and receive automated detection outputs, including lesion localization and confidence predictions.

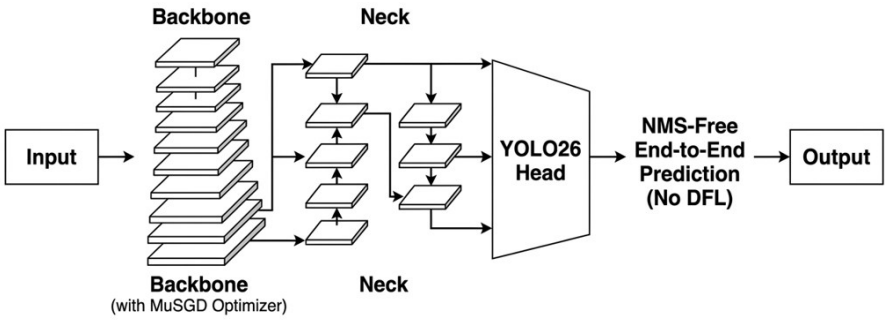

Fig. 2: YOLO26 Architecture

2.6 Evaluation Metrics

The performance of the proposed YOLO26 liver cancer detection framework was evaluated using Precision, Recall, F1-Score, and Mean Average Precision (mAP). These metrics were selected because they provide comprehensive assessment of both classification accuracy and object localization performance in detection systems (Sidi *et al*., 2026; Li, 2024).

Precision measures the proportion of correctly identified liver cancer lesions among all predicted lesion detections and evaluates the model's ability to minimize false-positive predictions. This was achieved using equation 1

$$Precison = \frac{TP}{TP+FP} \quad (1)$$

where TP represents True Positives and FP represents False Positives.

Recall (equation 2) measures the proportion of actual liver cancer lesions correctly detected by the model and reflects the sensitivity of the detection framework.

$$Recall = = \frac{TP}{TP+FN} \quad (2)$$

where FN represents False Negatives.

The F1-Score provides a balanced assessment of Precision and Recall and is calculated according to equation 3

$$F! = 2 \times \frac{Recall \times Precision}{Reca;; + Precision} \quad (3)$$

Precision (mAP) evaluates overall object detection performance by measuring the quality of predicted bounding boxes across different confidence thresholds and Intersection over Union (IoU) values. It remains one of the most widely accepted performance indicators for object detection models and provides a comprehensive measure of localization and classification effectiveness (Review & Previous, 2025; Sapkota *et al*., 2026).

3.0 Results and Discussion

3.1 Resukts

3.1.1 Quantitative Performance Evaluation

The quantitative performance metrics obtained from the trained YOLO26 model are presented in Fig. 3. The model achieved a Precision of 0.9600, Recall of 0.9257, F1-Score of 0.9425, and Mean Average Precision (mAP@0.5) of 0.9600. These results indicate that the proposed model demonstrated excellent capability in identifying and localizing malignant liver lesions within CT images.

The high precision value indicates that the model generated very few false-positive predictions, thereby improving the reliability of liver lesion identification. Similarly, the high recall value demonstrates the model's effectiveness in detecting actual cancerous lesions, reducing the likelihood of missed detections. The F1-score further confirms a balanced trade-off between precision and recall, while the mAP@0.5 value reflects strong overall object detection and localization performance. The obtained results compare favorably with previously reported YOLO-based liver tumor detection models and other deep learning approaches in medical imaging (Li, 2024; Sidi *et al*., 2026; Li, 2025). The quantitative performance of the proposed YOLO26 model is summarized in Fig. 3. The model achieved a Precision of 0.9600, Recall of 0.9257, F1-score of 0.9425, and mAP@0.5 of 0.9600, indicating strong detection and localization performance.

To further assess the detection capability of the proposed framework, the Precision–Recall (PR) curve is presented in Fig. 4. The curve demonstrates that the model maintained high precision across a wide range of recall values, indicating stable and reliable detection performance under varying confidence thresholds.

A Precision–Recall curve that remains close to the upper-right corner of the graph is generally indicative of a highly effective object detection system. The observed curve suggests that the YOLO26 model was capable of maintaining detection accuracy while simultaneously identifying a large proportion of true liver cancer lesions. This behavior is particularly important in medical diagnosis, where both false positives and false negatives can significantly affect clinical decision-making.

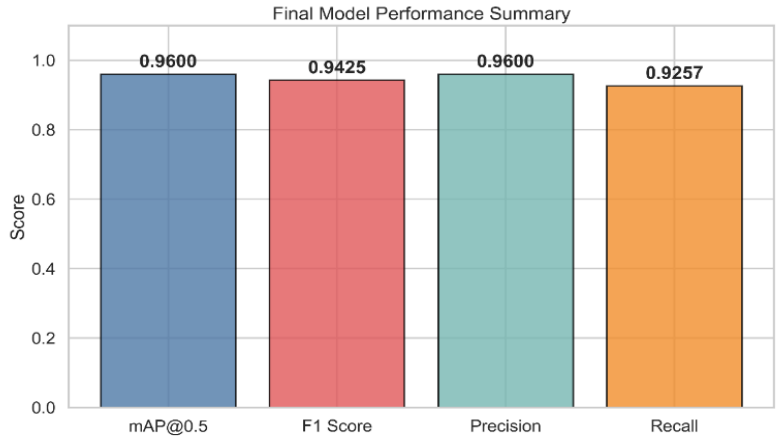

Fig. 3: Overall System Performance

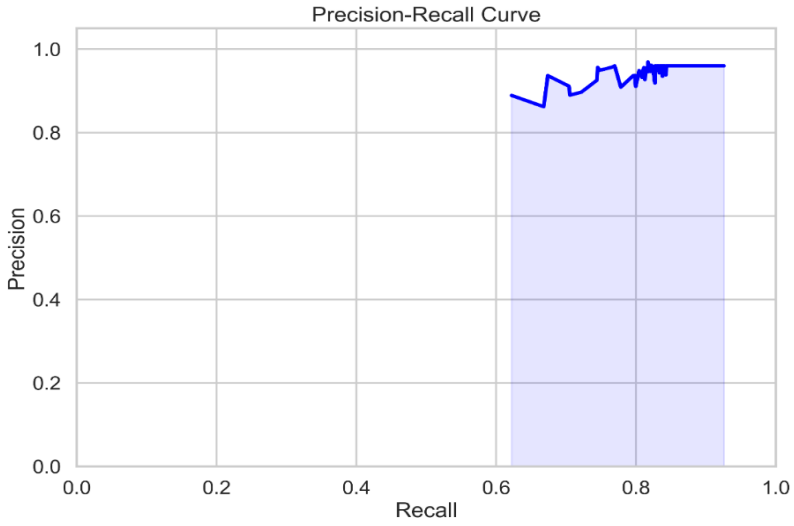

Fig. 4: Precision–Recall Curve of the

3.1.2 Proposed YOLO26 Framework

The relationship between the F1-score and confidence threshold is illustrated in Fig. 5. The curve shows that the model achieved its optimal F1-score at higher confidence levels, demonstrating a balanced relationship between precision and recall. The observed trend indicates that the model effectively minimized false-positive and false-negative predictions as the confidence threshold increased. This result further confirms the robustness of the proposed detection framework and its suitability for clinical liver cancer screening applications where diagnostic reliability is essential.

3.1.3 Training Dynamics and Convergence Analysis

The training performance of the YOLO26 model across 100 epochs is presented in Fig. 6. The figure illustrates the progression of the model's evaluation metrics throughout the training process.

The results reveal a gradual improvement in detection performance during the early training stages, followed by stabilization in the later epochs. This behavior indicates that the model successfully learned discriminative features associated with liver cancer lesions and

converged toward an optimal solution. The stable performance observed after convergence further suggests that the selected training parameters and optimization strategy were appropriate for the detection task.

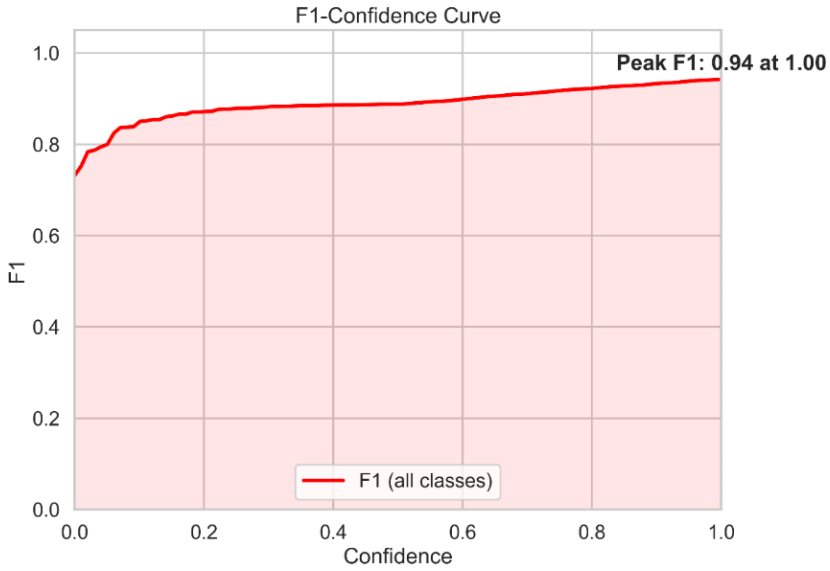

Fig. 5: F1-Score versus Confidence Threshold Curve

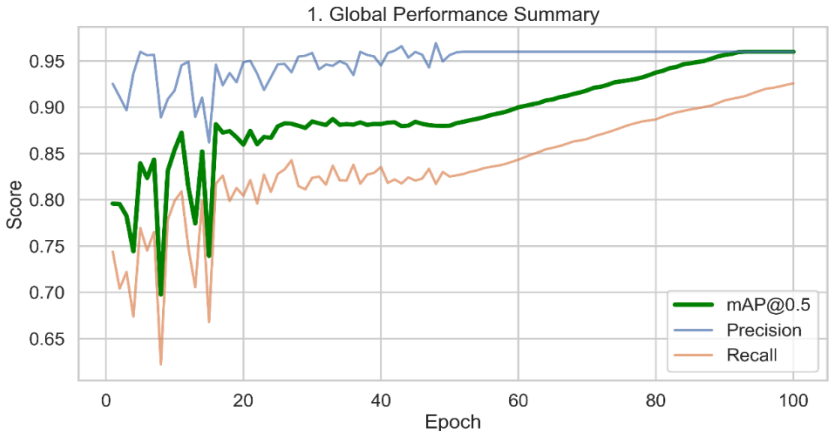

Fig. 6: Global Performance Evolution During Model Training

The training and validation loss curves are shown in Fig 7. Both curves exhibit a steady decline throughout the training process and remain closely aligned as training progresses. The similarity between the training and validation loss curves suggests that the model did not suffer from significant overfitting. Instead, the model maintained good generalization capability across unseen validation data. The consistent reduction in loss values indicates effective feature learning and stable optimization during the training process. These findings are consistent with previous studies that reported improved convergence characteristics and learning stability

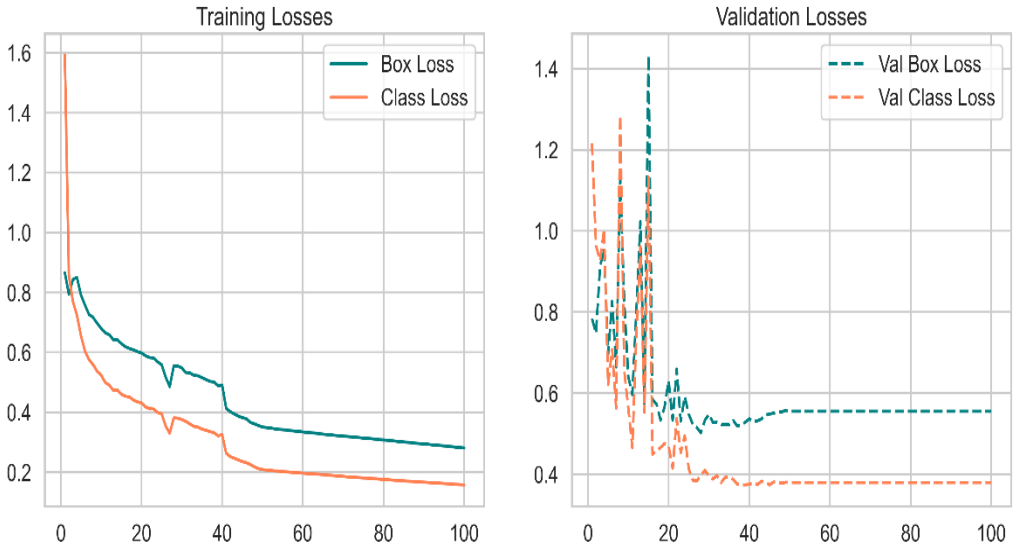

Fig. 7: Training and Validation Losses

The optimization schedule employed during training is presented in Fig. 8. The figure illustrates the gradual reduction of the learning rate throughout the training process. The decreasing learning rate enabled the model to make larger parameter updates during the initial training stages while allowing finer adjustments during later epochs. This adaptive optimization strategy contributed to stable convergence and improved detection performance. The observed relationship between learning rate reduction and performance improvement demonstrates the effectiveness of the selected optimization approach in enhancing model learning efficiency.

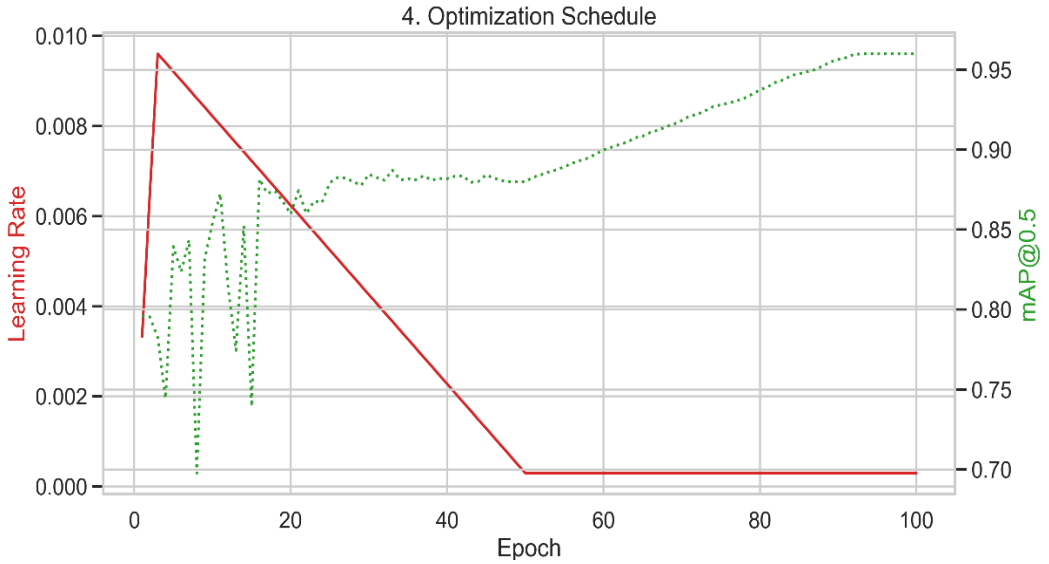

Fig. 8: Optimization Schedule

3.1.4 Qualitative Detection Result

The qualitative detection results produced by the trained YOLO26 model are presented in Fig. 9. The model successfully identified and localized liver cancer lesions across different CT scan samples, generating confidence scores ranging from approximately 0.96 to 0.97.

Visual inspection of the detection outputs revealed that the predicted bounding boxes closely corresponded to the annotated lesion regions, indicating accurate localization performance. The model was able to identify lesions of varying sizes and morphological characteristics, demonstrating its capability to learn meaningful representations of liver cancer patterns from CT images. The high confidence scores associated with the detected lesions further indicate that the model generated reliable predictions and maintained consistency across different test samples.

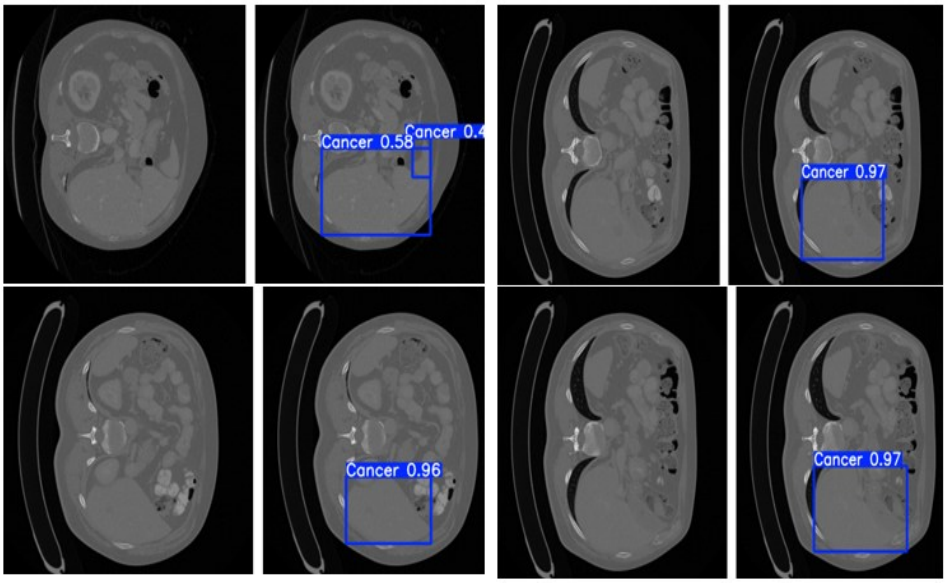

Fig. 9: Qualitative Effectiveness

These findings support the quantitative results obtained from the evaluation metrics and confirm the effectiveness of the proposed YOLO26 framework for automated liver cancer detection.

3.4 Deployment and Real-Time Inference Validation

To evaluate the practical applicability of the proposed framework, the trained YOLO26 model was integrated into a Gradio-based deployment environment. The deployment interface and sample inference results are presented in Fig. 10. The deployment system successfully processed previously unseen CT images and generated real-time detection outputs with corresponding lesion localization and confidence scores. The ability to perform rapid inference while maintaining high detection accuracy demonstrates the feasibility of deploying the proposed framework as a computer-aided diagnostic tool for liver cancer screening and clinical decision support.

The Gradio interface provided a user-friendly environment that allowed users to upload CT images and visualize detection results without requiring specialized programming expertise. This practical deployment capability enhances the potential translational value of the research and supports the integration of artificial intelligence-based diagnostic systems into healthcare workflows.

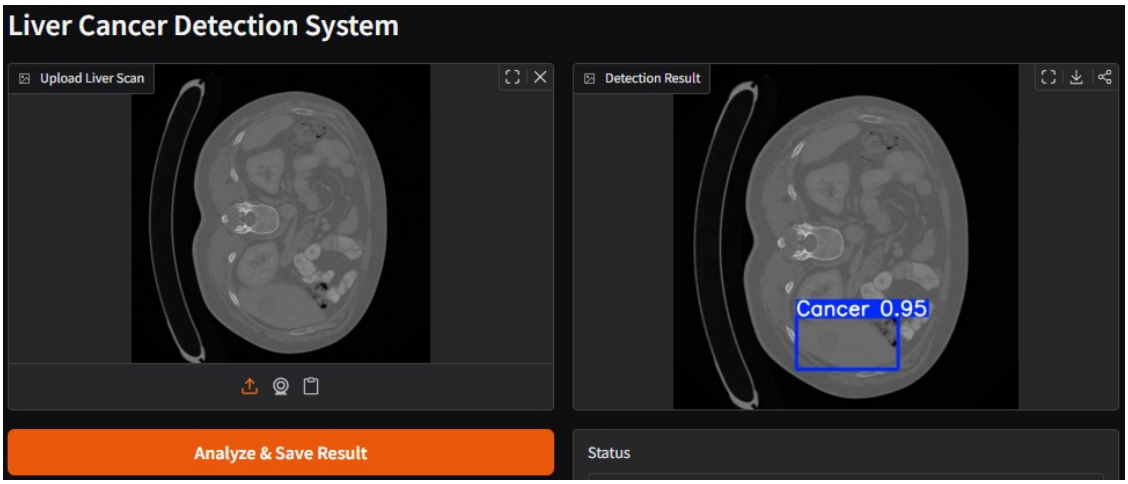

Fig. 10: Gradio Deployment

3.2 Discussion of Results

The results obtained from this study demonstrate that the proposed YOLO26-based framework is highly effective for automated liver cancer detection and localization using Computed Tomography (CT) images. The model achieved a Precision of 0.9600, Recall of 0.9257, F1-Score of 0.9425, and Mean Average Precision (mAP@0.5) of 0.9600, indicating excellent performance in identifying and localizing malignant liver lesions. These findings suggest that the model was capable of accurately distinguishing cancerous tissues from surrounding liver structures while maintaining a low rate of false-positive and false-negative detections. The high mAP value further confirms the robustness of the proposed framework in accurately predicting lesion boundaries and spatial locations within complex CT images.

The findings directly address one of the major challenges identified in the literature, namely the difficulty of detecting liver tumors in heterogeneous and low-contrast CT images. Previous studies reported that image noise, poor tissue differentiation, structural variability, and low contrast between healthy and cancerous tissues often reduce diagnostic accuracy and hinder reliable lesion detection (Moghimhanjani & Taghavirashidizadeh, n.d.; Rahoma *et al*., 2024; Tatar *et al*., 2025). In the present study, the consistently high performance metrics and stable detection outputs indicate that the YOLO26 architecture was able to effectively learn discriminative features associated with malignant liver lesions despite these imaging challenges. Furthermore, the close alignment between training and validation loss curves suggests that the model achieved good generalization capability with minimal overfitting, thereby enhancing its reliability for unseen data.

One of the primary objectives of this study was to evaluate the capability of YOLO26 to improve lesion localization while maintaining high detection accuracy. The results indicate that this objective was successfully achieved. Unlike conventional computer-aided diagnostic approaches that often perform segmentation, feature extraction, and classification as separate processes, the proposed framework utilized a single-stage end-to-end object detection strategy that simultaneously performed lesion localization and classification. This integrated approach reduced computational complexity while maintaining high detection performance. Similar studies have demonstrated the effectiveness of YOLO-based architectures in medical image analysis; however, many existing systems relied on complex multi-stage or ensemble learning frameworks that

increased computational requirements and reduced deployment flexibility (Vamsy *et al*., 2026; Badrawy *et al*., 2024). By contrast, the YOLO26 architecture provided a streamlined detection pipeline capable of delivering accurate predictions without requiring multiple interconnected models.

Another important challenge identified in previous studies relates to the detection of small liver tumors and the maintenance of localization consistency. Small lesions often exhibit subtle visual characteristics and are easily overlooked in CT images, particularly under low-contrast imaging conditions (Li, 2025; Huang, 2024). The qualitative detection results obtained in this study demonstrated that the proposed model successfully localized suspicious liver lesions with confidence scores ranging between 0.96 and 0.97 across different CT samples. This performance can be attributed to the use of high-resolution input images and the multi-scale feature aggregation mechanism incorporated within the YOLO26 architecture. Multi-scale feature learning enabled the model to capture both fine-grained local details and broader contextual information, thereby improving its ability to detect lesions of varying sizes. These findings are consistent with previous studies that reported improved detection performance when multi-scale feature extraction techniques were employed for medical object detection tasks (Li, 2025).

The study also addressed limitations related to robustness and model generalization that have been highlighted in recent liver cancer detection research. Previous investigations reported that several deep learning models experienced performance degradation when applied to datasets containing diverse pathological characteristics and imaging conditions (Alqaralleh *et al*., 2026; Huang *et al*., 2024). In the present study, the strong quantitative performance metrics, stable convergence behavior, and successful detection of lesions across different CT samples suggest that the YOLO26 model was capable of learning generalized feature representations. The enhanced feature extraction capabilities and architectural improvements introduced in YOLO26 likely contributed to its ability to maintain consistent detection performance across heterogeneous imaging conditions (Sapkota *et al*., 2026).

An additional contribution of this study is the successful implementation of a Gradio-based deployment environment for real-time inference. The deployment framework demonstrated the ability to process previously unseen CT images and generate rapid detection outputs with corresponding lesion localization and confidence scores. This capability highlights the practical applicability of the proposed system beyond experimental evaluation. Real-time deployment is particularly important in clinical environments where rapid decision-making and diagnostic support are essential. The integration of an interactive deployment interface further improves accessibility and demonstrates the potential of the framework for future clinical decision-support applications (Sani *et al*., 2026).

Overall, the findings of this study indicate that the proposed YOLO26-based liver cancer detection framework effectively addressed several limitations identified in previous research, including localization inconsistency, poor small-lesion detection, high computational complexity, and limited deployment flexibility. The combination of high detection accuracy, strong localization performance, stable learning behavior, and successful real-time deployment confirms the suitability of YOLO26 as a robust computer-aided diagnostic framework for liver cancer detection using CT images. These results contribute to the growing body of knowledge on artificial intelligence-assisted medical imaging and provide evidence supporting the

adoption of advanced object detection architectures for improved cancer diagnosis and clinical decision-making.

5.0 Conclusion

This study presented a YOLO26-based deep learning framework for automated liver cancer detection and localization using CT scan images. The proposed system was designed to address challenges associated with low-contrast liver tissues, inconsistent lesion localization, and poor small tumor detection commonly reported in existing liver cancer detection approaches. Using approximately 12,000 annotated CT images, the model was trained and evaluated within an end-to-end object detection framework capable of simultaneous lesion localization and classification. Experimental evaluation demonstrated strong detection performance, with the model achieving a Precision of 0.9600, Recall of 0.9257, F1-score of 0.9425, and mAP@0.5 of 0.9600. The results further showed stable convergence during training, minimal overfitting, and effective detection consistency across different CT image samples. In addition, the qualitative detection outputs confirmed the model's ability to accurately localize suspicious liver lesions with high confidence values, including smaller lesions that are often difficult to detect in medical imaging environments.

Compared with several existing studies reviewed in this research, the proposed framework provided improved localization consistency and reduced architectural complexity through its single-stage YOLO26 detection mechanism. The integration of a Gradio-based deployment environment also demonstrated the practical real-time inference capability of the system on unseen CT images. Overall, the findings confirm that YOLO26 is a reliable and efficient computer-aided approach for automated liver cancer detection and has strong potential for future medical imaging and clinical diagnostic support applications.

6.0 References

Alqaralleh, B. A. Y., Alksasbeh, M. Z., Kulakli, A., & Zreikat, A. I. (2026). An intelligent healthcare framework for hepatocellular carcinoma diagnosis based on aggregated learners from biomedical data utilising explainable artificial intelligence. *Scientific Reports*, *16*, Article 9357. https://doi.org/10.1038/s41598-026-39871-z

Amin, N., Anwar, J., Sulaiman, A., Naumova, N. N., & Anwar, N. (2025). Hepatocellular carcinoma: A comprehensive review. *Diseases*, *13*(7), Article 207. https://doi.org/10.1038/diseases13070207

Badrawy, N., Khalil, A. T., & Amer, H. M. (2024). Liver cancer detection using artificial intelligence. *Journal of Medical Imaging and Health Informatics*, 14(3), pp. 412–433. https://doi.org/10.1166/jmihi.2024.1021

Dadjouy, S. (2025). Gallbladder cancer detection in ultrasound images based on YOLO and Faster R-CNN. *Biomedical Signal Processing and Control*, 92(1), Article 106012. https://doi.org/10.1016/j.bspc.2025.106012

Hu, B. (2026). Global advances in hepatocellular carcinoma research and therapy in 2025. *Cancer Innovation*, 5(2), Article e70059. https://doi.org/10.1002/cai2.70059

Huang, C. (2024). Liver ultrasound imaging lesion detection based on YOLO. *International Journal of Engineering Technologies and Management Research*, 11(7), pp. 8–13. https://doi.org/10.29121/ijetmr.v11.i7.2024.1475

Huang, S., Nie, X., Pu, K., Wan, X., & Luo, J. (2024). A flexible deep learning framework for liver tumor diagnosis using variable multi-phase contrast-enhanced CT scans. *Journal of Cancer Research and Clinical Oncology*, 150(10), pp. 1–12. https://doi.org/10.1007/s00432-024-05977-y

Karabağ, B., Ayturan, K., & Hardalaç, F. (2026). Liver tumor segmentation with deep learning: A comparative analysis of CNN-, Transformer-, and YOLO-based models on the ATLAS MRI. *Diagnostics*, 16(5), Article 649. https://doi.org/10.3390/diagnostics16050649

Li, X. (2025). PCA-YOLO: A small liver tumor detection model with patch-contrastive attention. *Computers in Biology and Medicine*, 182(1), Article 109123. https://doi.org/10.1016/j.compbiomed.2025.109123

Li, Z. (2024). Advanced liver tumor detection in abdominal CT scans using modified YOLOv8. *ACM Transactions on Computing for Healthcare*, 1(1), Article 3719428. https://doi.org/10.1145/3719384.3719428

Luu, M. H., van Walsum, T., Mai, H. S., & Franklin, D. (2024). Automatic scan range for dose-reduced multiphase CT image of the liver utilizing CNNs and Gaussian models. *Medical Image Analysis*, 91(1), Article 103012. https://doi.org/10.1016/j.media.2024.103012

Moghimhanjani, M., & Taghavirashidizadeh, A. (2022). Analysis of liver cancer detection based on image processing. *arXiv preprint*, arXiv:2207.08032. https://doi.org/10.48550/arXiv.2207.08032

Nakao, Y., Tokunaga, T., Sato, M., & Tanaka, K. (2024). Investigation of deep learning model for predicting immune checkpoint inhibitor treatment efficacy on contrast-enhanced computed tomography images of hepatocellular carcinoma. *Scientific Reports*, 14(1), Article 5707. https://doi.org/10.1038/s41598-024-57078-y

Osman, A. B. (2026). Quantum machine learning approaches for medical image analysis: Methods and diagnostic applications. *Quantum Information Processing*, 25(1), Article 104. https://doi.org/10.1007/s11128-026-04210-x

Rahoma, K. H., Ibrahim, H. A. A., & Massoud, M. A. (2024). Automated detection of primary liver cancer using different deep learning approaches. *Journal of Radiation Research and Applied Sciences*, 43(1), pp. 112–124. https://doi.org/10.1016/j.jrras.2024.100812

Previous, T. (2025). YOLO evolution: A comprehensive benchmark and architectural review of YOLOv12, YOLO11, and their previous versions. IEEE Access, 13(1), pp. 10214–10235. https://doi.org/10.1109/ACCESS.2025.3421098

Sani, A., Hassan, Z. L., Balarabe, A. T., & Muhammad, J. M. (2026). Machine learning approaches for credit card fraud detection: A comparative study of logistic regression and K-nearest neighbors. Caliphate *Journal of Science and Technology CaJoST*, 14(2), pp. 24–34.

Sani, A., Yauri, B. A., Garba, M., & Balarabe, A. T. (2026). A YOLO26-based human detection framework for high-entropy disaster environments. *African Journal of Computing & ICT*, 14(1), pp. 157–167.

Sankuru, D. F., & Gujjarlapudi, R. (2026). Artificial intelligence in oncology: From multimodal risk prediction to equitable cancer prevention. *International Journal of Scientific Research*, 15(2), pp. 18–20. https://doi.org/10.36106/ijsr/2277018

Sapkota, R., Harsha, R., & Ajay, C. (2026).

YOLO26: Key architectural enhancements and performance benchmarking for real-time object detection. *Vision Processing Letters*, 8(1), pp. 1–15. https://doi.org/10.1016/j.vpl.2026.100412

Shen, Y., Zhang, L., & Wu, P. (2025). The role of artificial intelligence in ultrasonographic diagnosis of liver cancer: Current status and future perspectives. *Gastroenterology & Endoscopy*, 3(4), pp. 241–250. https://doi.org/10.1016/j.gande.2025.09.002

Sidi, S. A., Balarabe, A. T., Sani, A., & Yauri, B.

A. (2026). YOLOv8-based deep learning system for liver tumor detection. *Journal of Science and Technology Research*, 13(4), pp. 293–306.

Sun, L. (2025). FALS-YOLO: An efficient and lightweight method for automatic brain tumor detection and segmentation. *IEEE Transactions on Medical Imaging*, 44(2), pp. 512–523. https://doi.org/10.1109/TMI.2025.3389102

Tatar, O. C., Utkan, N. Z., Hospital, G. C., & Surgery, G. (2025). Diagnostic performance of deep learning applications tomography imaging. *The Turkish Journal of Gastroenterology*, 36(2), pp. 124–130. https://doi.org/10.5152/tjg.2024.24538

Vamsy, K., Pradesh, A., Pradesh, A., Godavari, & Lakshmaiah, K. (2026). CT-LiverNet: An efficient deep learning model for liver lesion segmentation and diagnosis. *International Journal of Intelligent Systems*, 104(1), pp. 268–282. https://doi.org/10.1002/int.2026104

Wu, Z., Xia, F., Wang, W., Zhang, K., Fan, M., &

Lin, R. (2024). Worldwide burden of liver cancer across childhood and adolescence, 2000–2021: A systematic analysis of the Global Burden of Disease Study 2021. eClinicalMedicine, 75(1), Article 102765. https://doi.org/10.1016/j.eclinm.2024.102765

Zhou, J., Xia, Y., Xun, X., & Yu, Z. (2025). Deep learning-based detect-then-track pipeline for treatment outcome assessments in immunotherapy-treated liver cancer response evaluation criteria in solid tumors. *Journal of Imaging Informatics in Medicine*, 38(1), pp. 380–393. https://doi.org/10.1007/s10278-024-01132-8

Declarations

Ethics Approval and Consent to Participate

This study utilized publicly available and anonymized CT image datasets. Therefore, ethical approval and informed consent were not required.

Consent for Publication

All authors have read and approved the final manuscript and consented to its publication.

Availability of Data and Materials

The datasets and materials used in this study are available from publicly accessible sources. Additional information may be obtained from the corresponding author upon reasonable request.

Funding

The authors received no specific funding for this research.

Competing Interests

The authors declare that they have no competing financial or personal interests that could have influenced the work reported in this study.

Author Contributions

Muhammad Jamilu Muhammad conceptualized the study, collected and preprocessed the data, developed and trained the YOLO26 model, performed the experiments, analyzed the results, and drafted the manuscript. Anas Tukur Balarabe supervised the research, contributed to the

study design and methodology, and critically reviewed the manuscript. Bashar Aliyu Yauri assisted with data validation, model evaluation, and result interpretation. Hassan Umar Suru contributed to the literature review, software implementation, and manuscript editing. Abdulrashid Sani provided technical guidance, validated the findings, reviewed the manuscript, and coordinated the overall research activities. All authors read and approved the final version of the manuscript.